Does capsule quality matter? A comparison study between spherical microphone arrays using different types of omnidirectional capsules

Simeon Delikaris-Manias, Vincent Koehl, Mathieu Paquier, Rozenn Nicol,
Jérôme Daniel

▶ **To cite this version:**

HAL Id: hal-00612849

https://hal.univ-brest.fr/hal-00612849

Submitted on 8 Nov 2011

"DOES CAPSULE QUALITY MATTER?" A COMPARISON STUDY BETWEEN SPHERICAL MICROPHONE ARRAYS USING DIFFERENT TYPE OF OMNIDIRECTIONAL CAPSULES.

Simeon Delikaris-Manias[†], Vincent Koehl[†], Mathieu Paquier[†], Rozenn Nicol[‡], Jerome Daniel[‡]

[†]European Center of Virtual Reality
UEB - UBO – LISyC EA 3883
29200 Brest, France
delikaris@enib.fr
{vincent.koehl, mathieu.paquier}@univ-brest.fr

[‡]Orange Labs
TECH/OPERA
22307 Lannion, France
{rozenn.nicol, jerome.daniel}@orange-ftgroup.com

ABSTRACT

This study presents an objective comparison between two rigid spherical microphone arrays of the exact same size but differing by the type of capsules. An analysis of the simulations and the encoding process is presented and known limitations of the spherical arrays are discussed such as the degraded reconstruction of the spherical harmonics due to the size of the sphere and the size and number of the capsules.

1. INTRODUCTION

There is a number of applications of spherical microphone arrays such as measuring acoustic characteristics of rooms, teleconferencing, recording spatial audio and in general cases where an optimal reconstruction of the soundfield is required. Recording audio using microphone arrays for surround purposes is a process which involves designing the actual arrays, placing the sensors in the right place, studying the diffraction properties of the enclosure that hosts the sensors and developing the complex signal processing techniques in order to encode the acquired signals to a usable format. Encoding microphone outputs to a set of spherical harmonics components provides enough information to then decode it to any number of speakers for reproduction of the prerecorded material. First microphone arrays were developed and constructed in the 70's when the first tetrahedron array prototype was proposed by Craven and Gerzon [1]. Since then there were various attempts in designing more advanced arrays with wider reconstruction area and more accurate representation of spatial sounds. Several studies have focused on microphone array construction including first or higher order, spherical and non spherical microphone arrays; however generating a high-resolution spatial audio acquisition is still a challenge. Examples of such studies analyzing the general performance of spherical and non spherical microphone arrays can be found in [2], [3], [4] and [5] but there is less attention that evaluates the role of capsule quality in microphone array construction. In this paper a comparison between spherical microphone arrays using different capsules is presented and analyzed.

The aim of this paper is to present a study of the performance of two spherical microphone arrays with different capsules and determine whether the choice of the capsule affects the overall quality of the spatial encoding; specifically, if the resulting timbre problems that are often reported by sound engineers are due to artifacts caused by the signal processing or the transducers used in the microphone array. It is investigated to what extent a capsule of assumed lower quality is able to achieve accurate extraction of the spherical harmonic components. The performance of each spherical array is characterized by evaluating the reconstructed spherical harmonics.

2. THEORY

2.1. Acquiring spatial audio using spherical microphone arrays

The starting point of analyzing a sound field with a spherical microphone array is the Fourier-Bessel series of the acoustic pressure:

$$p(r, \theta, \phi) = \sum_{m=0}^{\infty} \sum_{n=-m}^{m} B_{mn}^{\sigma} j_m(kr) Y_{mn}^{\sigma}(\theta, \phi), \quad (1)$$

where r is the radius, θ the azimuthal angle, ϕ the elevation angle, j_m the mth spherical Bessel functions and Y are the so called spherical harmonics. Details on the properties of the Bessel functions and the spherical harmonics can be found in Williams [6] and Abhayapala et al. [7]. A soundfield can be defined at any position by calculating the spherical harmonic components B_{mn} [8]. For a given sensor on the surface of a rigid sphere placed at azimuth θ_1 and elevation ϕ_1 equation (1) can be written as:

$$p(R, \theta_1, \phi_1) = \sum_{m=0}^{\infty} \sum_{n=-m}^{m} B_{mn}^{\sigma} W_m(kR) Y_{mn}^{\sigma}(\theta_1, \phi_1), \quad (2)$$

where R is the radius of the sphere and $W_m(kR)$ are the weightings that describe the sensor directivity [8]. If the pressure is

measured with a finite number of sensors Q on the surface of a rigid sphere at the angles θ_Q and ϕ_Q, equation (2) can be written in a matrix form as:

$$p_Q(R, \theta_Q, \phi_Q) = Y_{mn}^{\sigma}(\theta_Q, \phi_Q)W_m(kR)B_{mn}^{\sigma}. \quad (3)$$

In an extended simplified matrix form equation (3) can be re-written as:

$$\begin{bmatrix} p_1 \\ \vdots \\ p_Q \end{bmatrix} = \begin{bmatrix} Y_{00}^1 & \cdots & Y_{mn}^1 \\ \vdots & \ddots & \vdots \\ Y_{00}^1 & \cdots & Y_{mn}^1 \end{bmatrix} \begin{bmatrix} W_0 & \cdots & 0 \\ \vdots & \ddots & \vdots \\ 0 & \cdots & W_m \end{bmatrix} \begin{bmatrix} B_{oo}^1 \\ \vdots \\ B_{mn}^{\sigma} \end{bmatrix}$$

$$(4)$$

Hence, the higher order ambisonic components b_{mn} can be estimated by using the signals received by the Q sensors. From equation (4) we can obtain these components by inverting W and Y:

$$B = eq(W^{-1})pinv(Y)p_Q, \quad (5)$$

where p_Q are the microphone signals, $pinv(Y)$ the Moore-Penrose pseudo-inversion of Y and $eq(W^{-1})$ the regularized inverse matrix of the radial weightings W.

2.2. Limitations and spatial aliasing

There are physical limitations in the construction of a spherical microphone array. There is a trade-off between the performances at low and high frequencies. A large radius array is able to handle low frequencies due to the wavelength but it will produce spatial aliasing, an error in estimating high frequencies [9]. Spatial aliasing occurs mainly due the discrete arrangement of microphones on the sphere. The aliasing frequency f_{al} can be determined by the Shannon criterion as mentioned in Moreau et al. [2] and is the highest frequency that the array can deliver without the aliasing effect to take place:

$$f_{al} = \frac{c}{2R\gamma}, \quad (6)$$

where c is the speed of sound, R the array radius and γ the maximum angle between the sensors.

3. EXPERIMENTAL ARRANGEMENT AND PROCEDURE

3.1. Array Construction

Two spherical microphone array prototypes have been designed. Each array consists of eight omnidirectional capsules. The two sets of capsules that were fitted in each array differ by the membrane size. Directivity measurements of each capsule have been carried out to quantify these differences. The performance of each capsule was measured while they were mounted on a sphere. Each prototype required a specific design since it hosts capsules different in size. The eight capsules were arranged in the horizontal plane every 45^0, hence the spatial sampling takes place in 8 positions on a sphere. In theory this means that the specific spherical arrays is able to acquire a third order two-dimensional soundfield (limited to the horizontal plane) and it is possible to calculate up to seven spherical harmonic components.
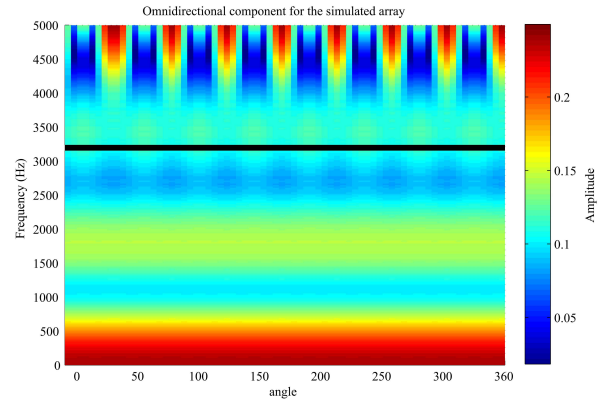

Figure 1: Simulated omnidirectional component.

3.2. Simulations

The first step in designing the microphone array prototypes is to use simulations to virtually test the array under construction. Specifically, simulations are used in order to determine the optimal size of the sphere that will host the capsules. The performance of each virtual spherical array is estimated. Upon successful simulation the two prototypes are built up.

Due to the size of the large membrane capsule used in one of the two arrays, the minimum radius of that array that could accommodate the large membrane capsules was 8cm. The simulations revealed that the aliasing frequency for the specific radius would be at approximately 3.2Hz. This is shown in Fig. 1 where the omnidirectional spherical component $W = B_{00}^{+1}$ is plotted for the frequency range between 20Hz and 5kHz and the angle between 0° and 360°. It can be observed that above the frequency of 3.2kHz, where the black line is plotted, level changes (that is indicated by the change of color), which is not a characteristic of the omnidirectional component and it proves the fact that spatial aliasing start occurring at that frequency. It should be noted that the virtual microphones in the simulation are dimensionless microphones.

3.3. Free field measurements

Both arrays were measured under free field conditions in the anechoic chamber of Orange Labs in Lannion. Each array was mounted in the center of a Brüel and Kjær turntable. The speaker under use was a Cabasse sphere amplified by a Denon PMA-S1. An RME Octamic II amplified the microphone signals and an RME Fireface 800 was used as the main audio interface. The setup inside the anechoic chamber is shown in Fig. 2 (a) and the two prototypes are shown in Fig. 2 (b) and (c) for the small and large membrane capsule array respectively.

The impulse response measurements were performed by feeding the loudspeaker with a sine sweep signal of four seconds from 22Hz up to 22kHz at 44.1kHz and then deconvolving the acquired signal from the eight microphones with the inverse of the original sine sweep. This process was repeated for every 5° until the microphone reached the initial position. This led to 73 measurements where the last measurement was compared to the first measurement to determine the accuracy of the turntable. The turntable was controlled through the Matlab environment.
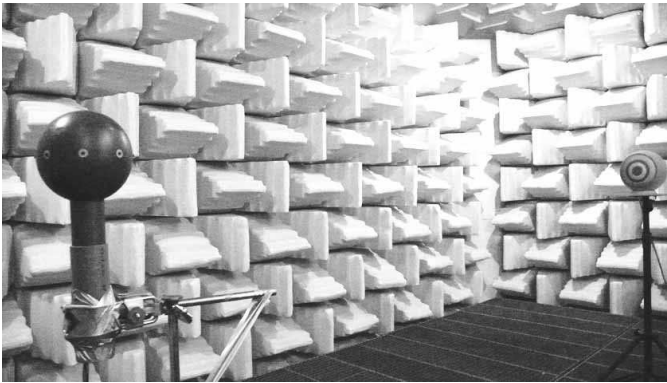
(a) Setup inside the anechoic chamber
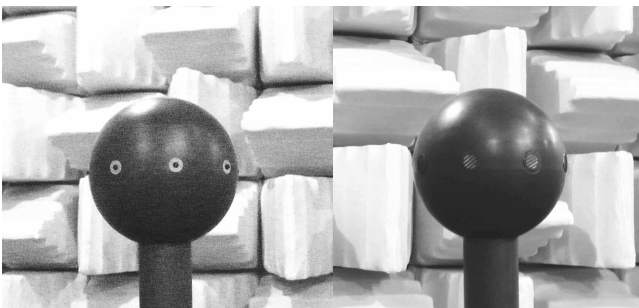
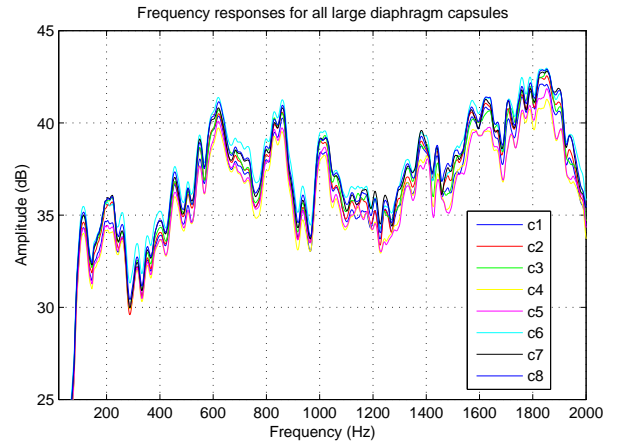(b) Small membrane capsules   (c) Large membrane capsules

Figure 2: Setup inside the anechoic chamber in Lannion (a) and two microphone arrays with small and large membrane capsules (b),(c) respectively.

(a) Large membrane

(b) Small membrane

Figure 3: Frequency response for all the capsules at the frontal position facing the loudspeaker.
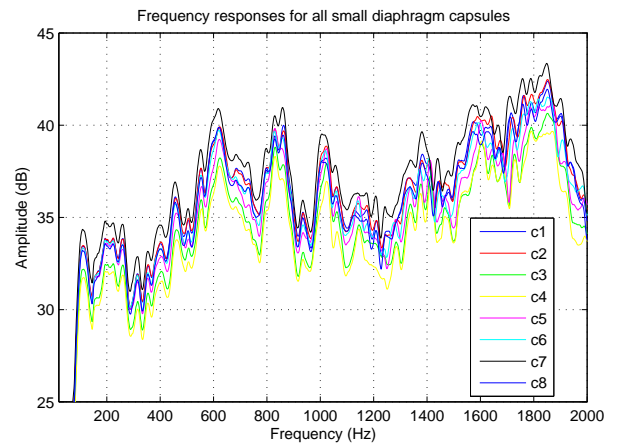
3.4. Capsule Comparison

Ideally, the capsules that are mounted on each microphone array should be perfectly matched but according to the measurements this is not the case. Frequency responses show that there is an average difference of approximately 3dB between the large membrane capsules and approximately 4dB for the small membrane capsules (the small membrane capsules were matched by the manufacturer in pairs). This is shown in Fig. 3 (a) and (b) where the frequency responses are plotted on the same graph for large and small capsules respectively. These responses have been measured when each capsule was at the frontal position of the array facing the loudspeaker.

The impulse responses for both spherical arrays for a frontal capsule are shown in Fig. 4 in logarithmic scale. This figure provides information about the signal to noise ratio. The noise floor is shown with the two black lines for both the small and the large membrane capsule. The relative signal to noise ratio, which can be observed as the difference between the main peak of the impulse response and the noise floor, is approximately the same for both capsules. Specifically, it is 89dB for the small membrane capsules and 92dB for the large membrane capsules. The amplification of each capsule was set manually and approximately as the knobs of the of the RME Octamic II interface provide virtually continuous adjustments without steps. Exactly the same amplification setup was used for both sets of capsules.

Frequency responses for both capsules indicate that the large membrane capsule are more sensitive in low and high frequen-

cies as shown in Fig. 5. The frequency response of two reference signals is also shown, one on top of the sphere with the black line and one in the middle of the sphere with the sphere absent. These reference signals show the effect caused by the presence of the sphere. It should be noted that the level of the large membrane microphone was increased by 5dB in Fig. 5 so it can reveal easier the differences between the frequency responses.

The measurement of each spherical array from 0° to 360° for every 5° provides also information on the directivity pattern for each capsule. In Fig. 6 the directivity patterns for both types of capsules is shown at 500Hz, $1, 2$ and 3kHz. The main difference between the two directivity patterns is that the large membrane microphone are more sensitive at low frequencies and more directive at high frequencies. According to Epain and Daniel [8], where a simulation with different sized membranes is studied, directivity patterns were similar except for high frequencies where the large membrane microphone was more directive.
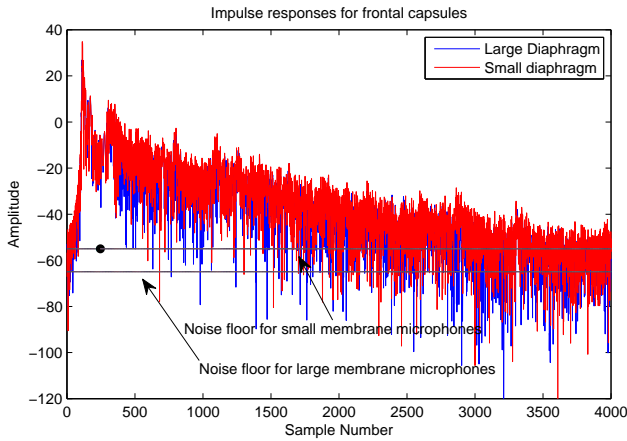
Figure 4: Impulse responses for small and large membrane capsules indicating the signal to noise ratio.

3.5. Processing the microphone signals

The process of constructing a spherical microphone array and obtaining the spherical harmonic components from the measured signals can be summarized briefly by the following steps:

- a distribution method is chosen for placing the capsules as uniformly as possible on the surface of the sphere. In this study this is quite trivial as there is only one way of distributing uniformly the eight capsules in the horizontal plane,

- sine sweeps are recorded for each capsule of the microphone array every 5° for a full rotation of the array (360°) so that the impulse response for each capsule can be obtained,

- calculation of the spherical harmonics matrix Y for the specific azimuthal position using an $N2D$ normalization scheme as described by Daniel [10],

- calculation of the gain matrix, which is the Moore-Penrose pseudo-inverse of matrix Y,

- calculation of the radial weightings and

- computation the spherical harmonic components according to equation (5).

4. RESULTS

The omnidirectional spherical harmonic component (W) is plotted in Fig. 7 (a) for the small membrane capsule and in (b) for the large membrane capsule. The x-axis indicates the angle which is between 0° and 360° and the y-axis the frequency. The color indicates the level which increases from blue to red. Spatial aliasing occurs at approximately 3.2kHz for both arrays. This value of 3.2Hz is indicated by the black line. It is clear from both figures that for frequencies above 4kHz, different angular positions cause a difference in level (indicated by red and blue color) which should not be the case for the omnidirectional component.

Fig. 8, 9 and 10 show the $X = B_{11}^{+1}$, $U = B_{22}^{+1}$ and $P = B_{33}^{+1}$ spherical harmonic component for the simulated array, the large membrane array and the small membrane array. This means one representative component per order: 1st (X),
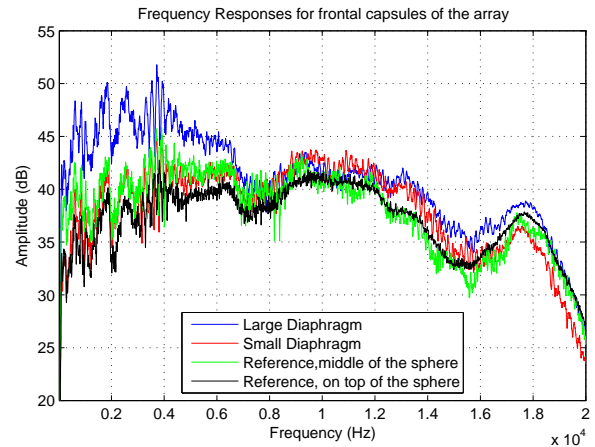

Figure 5: Frequency responses for small and large membrane capsules with two reference measurements. Blue line indicates the large membrane microphone, red line the small membrane, green line the reference signal measured in the center of the sphere and black line the reference signal on top of the sphere.

2nd (U) and 3rd (P). These figures are superimposed polar patterns for the frequency range between 20Hz and 3.5kHz with continuously varying frequency, where the frequency is in color scale. The main differences between the simulated array and the physical array are the artifacts that are visible for high frequencies, indicated by the red color. One might also observe that the calculated spherical harmonic components from the small membrane capsules produce more artifacts if compared with the components calculated form the large membrane capsules.

5. DISCUSSION

In our spherical harmonic component calculations there are errors related with:

- capsule positioning,

- capsule response mismatch,

- array positioning and

- reflections occurred during the measurements.

These errors also indicates the differences between the spherical harmonic components computed from the two measured arrays and the simulated array. The radius of the specific arrays results to a decreased bandwidth in the computed spherical harmonic components with spatial aliasing being present at 3.2kHz. Although these limitations affect the overall quality of spatial audio acquisition that these arrays can perform, this study mainly focuses on the comparison between the two different microphone membranes as the spatial aliasing error is the same for both arrays.

At this point it is not clear whether one of the large or the small membranes produce a higher quality spherical harmonic components and hence a higher quality reconstructed soundfield. Physical differences are not obvious and a further investigation through subjective evaluation will reveal if there is an actual preference between the two arrays and hence the two sets of membranes.

(a) Polar pattern at 500Hz

(b) Polar pattern at 1kHz

(c) Polar pattern at 2kHz
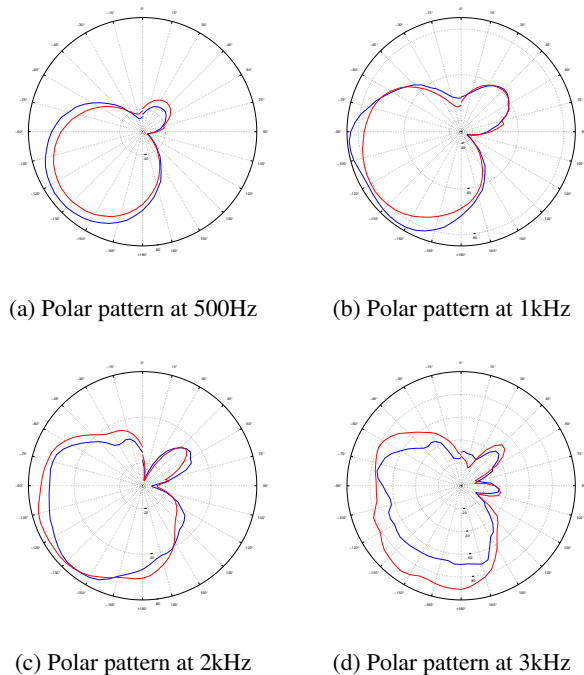
(d) Polar pattern at 3kHz

Figure 6: Polar patterns of one capsule from each array at the same position. The blue line indicates the large membrane capsule and red line the small membrane capsule.

(a) Small membrane

(b) Large membrane

Figure 7: Omnidirectional spherical harmonic component for two different capsules

6. CONCLUSIONS

Microphone arrays in general are a useful tool to investigate a sound field, to acquire the acoustical characteristics of a space or even use a spatially recorded material for virtual reality applications. In this paper we presented the construction of two identical spherical arrays where each one was fitted with a set of eight microphones. These two sets of microphones were of different membrane size. The comparison of the two arrays revealed differences in frequency responses as it was expected but little difference can be observed in the calculated spherical harmonic components. Further experiments will be crucial to determine whether the membrane size affects the overall quality of the reconstructed spherical harmonic components. Specifically, subjective experiments should be performed to demonstrate the ability of each array to handle accurate source position and timbre of acquired audio. Despite the relatively small bandwidth due to spatial aliasing the subjective experiments will reveal differences, if any between the two arrays. Upon successful completion of the subjective experiments a further experimentation could be the use of capsules that could fit in an array of a smaller diameter for an increased bandwidth of the reconstructed spherical harmonic components.

7. ACKNOWLEDGMENT

8. REFERENCES

[1] P. G. Craven and M. A. Gerzon, "Coincident Microphone Simulation Covering Three Dimensional Space and Yielding Various Directional Outputs", US Pattents, London, UK, 1977.

[2] S. Moreau, J. Daniel, and S. Bertet, "3D Sound Field Recording with Higher Order Ambisonics - Objective Measurements and Validation of a 4th Order Spherical Microphone", *AES 120th Convention*, Paris, France, 20-23 May, 2006.

[3] A. Parthy and C. Jin and A. V. Schaik, "Acoustic Holography with a Concentric Rigid and Open Spherical Microphone Array", *IEEE ICASSP 2009*, Taipei, Taiwan, 19-24 April, 2009.

[4] B. Rafaely, "Analysis and Design of Spherical Microphone Arrays", *IEEE Trans. on Speech and Aud. Proc.* , vol. 13, no. 1, pp. 135-143, 2005.

[5] J. Merimaa, "Applications of a 3-D Microphone Array", *AES 112th Convention*, Munich, Hermany, 10-13 May, 2002.

[6] E. Williams, *Fourier Acoustics: Sound Radiation and Nearfield Acoustic Holography*. London, UK: Academic Press, 1999.

[7] T. D. Abhayapala and D. B. Ward, "Theory and design of high order sound field microphones using spherical microphone arrays", *IEEE ICASSP 2002*, Orlando, Florida, 13-17 May, 2002.

[8] N. Epain and J. Daniel, "Improving Spherical Microphone Arrays", *AES 124th Convention*, Amsterdam, The Netherlands, 17-20 May, 2008.

[9] T. D. Abhayapala, R. Kenedy, and R. Williamson, "Spatial aliasing for near field sensor arrays", *IEEE Electronic Letters*, vol. 35, no. 10, pp. 764-765, 1999.

[10] J. Daniel, "Spatial Sound Encoding Including Near Field Effect: Introducing Distance Coding Filters and a Viable, New Ambisonic Format", *AES 23rd International Conference*, Copenhagen, Denmark, 23-25 March, 2003.
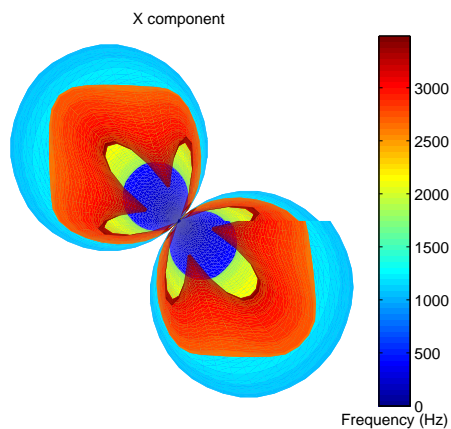
(a) Simulated component
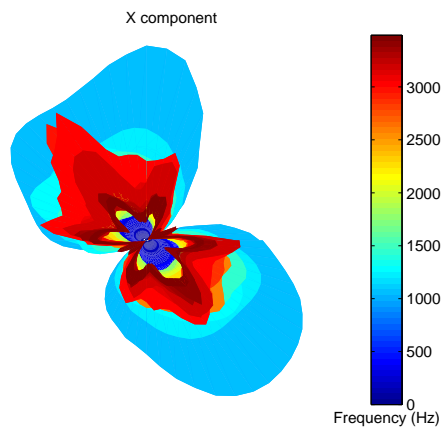
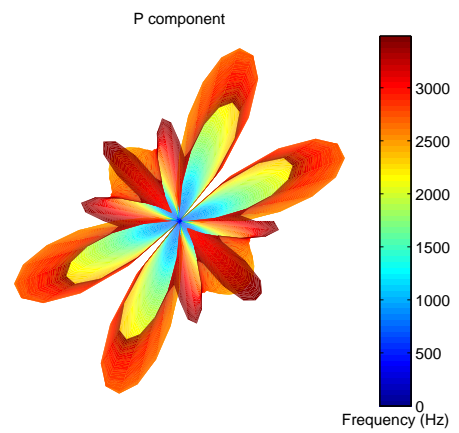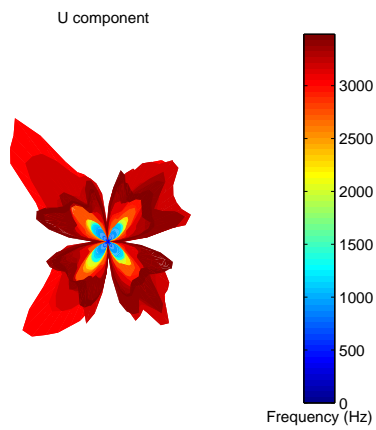(b) Large membrane component
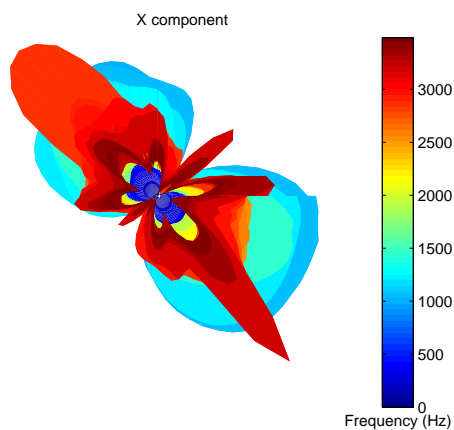
(c) Small membrane component
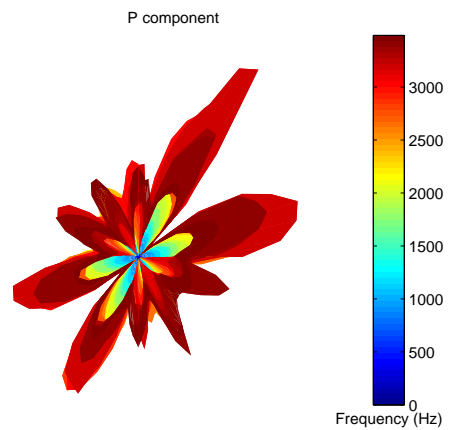
Figure 8: First order spherical harmonic component X
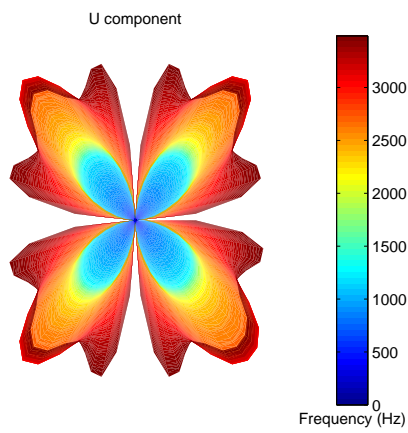
(a) Simulated component
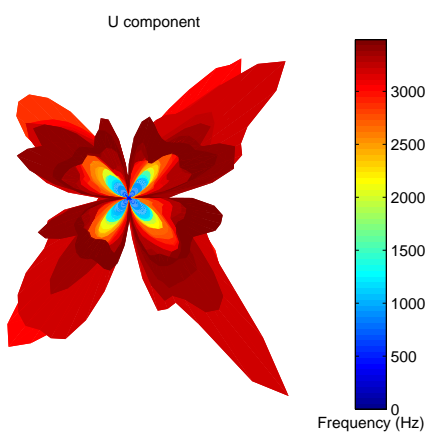
(b) Large membrane component
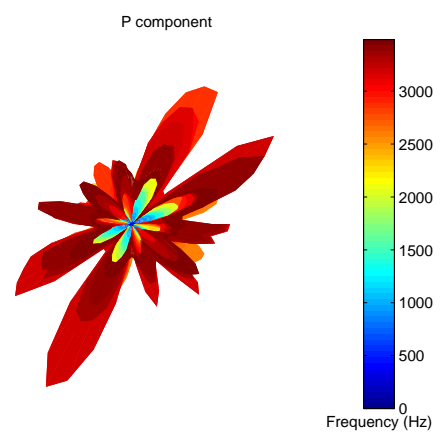
(c) Small membrane component

Figure 9: Second order spherical harmonic components U

(a) Simulated component

(b) Large membrane component

(c) Small membrane component

Figure 10: Third order spherical harmonic components P